



# Model-free control of a 3-DOF piezoelectric nanopositioning platform

José Manuel Rodriguez-Fortun, Frédéric Rotella, Jesus Alfonso, Francisco Javier Carrillo, Javier Orus

## ► To cite this version:

José Manuel Rodriguez-Fortun, Frédéric Rotella, Jesus Alfonso, Francisco Javier Carrillo, Javier Orus. Model-free control of a 3-DOF piezoelectric nanopositioning platform. Conference on Decision and Control, Dec 2013, Florence, Italy. pp.0. <hal-04086527>

**HAL Id: hal-04086527**

**<https://hal.science/hal-04086527v1>**

Submitted on 2 May 2023

**HAL** is a multi-disciplinary open access archive for the deposit and dissemination of scientific research documents, whether they are published or not. The documents may come from teaching and research institutions in France or abroad, or from public or private research centers.

L'archive ouverte pluridisciplinaire **HAL**, est destinée au dépôt et à la diffusion de documents scientifiques de niveau recherche, publiés ou non, émanant des établissements d'enseignement et de recherche français ou étrangers, des laboratoires publics ou privés.



HAL Authorization



## Open Archive Toulouse Archive Ouverte (OATAO)

OATAO is an open access repository that collects the work of Toulouse researchers and makes it freely available over the web where possible.

This is an author-deposited version published in: <http://oatao.univ-toulouse.fr/>  
Eprints ID: 10704

**To cite this version:**

Rodriguez-Fortun, José Manuel. and Rotella, Frédéric and Alfonso, J. and Carrillo, Francisco and Orus, Javier *Model-free control of a 3-DOF piezoelectric nanopositioning platform*. (2013) In: Conference on Decision and Control, 10 December 2013 - 13 December 2013 (Florence, Italy).

# Model-free control of a 3-DOF piezoelectric nanopositioning platform

J. M. Rodriguez-Fortun, F. Rotella, J. Alfonso, F. J. Carrillo and J. Orús

**Abstract**— A model-free controller is designed for a nanopositioning platform with three degrees of freedom. The system is specially difficult to control because of the coupling between the different movements and the hysteresis present in the piezoelectric actuators. The authors propose a control design methodology based on the so called *ultra-local* system description. The developed controller has been implemented and validated on a real test bench and it has proven a good performance in handling the nonlinearities and uncertainties present in the platform.

## I. INTRODUCTION

The control of nonlinear systems is a difficult task, normally requiring the experimental validation of complex mathematical models as a basis for the controller design. Given the difficulties arising from the identification of these representations, many efforts have been carried out in the last years for the development of model-free control techniques. In this connection, there are different methods that do not require detailed mathematical descriptions of the system, as some ILC approaches [8] (Iterative Learning Control), or the methods based on function approximators (FA). Different types of FA are: fuzzy representations [13], neural networks [2][1], splines, wavelets networks, trigonometric series or polynomials [15], among others. Of special interest are the *ultra-local* representations [3][4][5] because of their simplicity and direct control application. This method has been successfully used in electronic applications [10] or robotic devices [16][17], and has been applied in delayed and non-minimum phase systems [11][12].

In the current work, a controller based on the *ultra-local* representation is proposed for positioning a three-axis nanopositioning platform and it is experimentally proven its capability to handle the coupled effects between the actuation lines and the hysteresis of the piezoelectric actuators.

For the design of the model-free control, we propose a new design methodology that considers different estimation procedures for the main parameters of the controller.

In the next section, the nanopositioning system is described. In Section 3 the model-free controller is introduced, and the design methodology is presented in the Section 4. Its experimental performance is described in the Section 5 and the conclusions are summarized in the Section 6.

J. M. Rodriguez-Fortun, J. Alfonso and J. Orús are with the SISTRONIC group, Instituto Tecnológico de Aragón, Zaragoza, Spain  
e-mail:{jmrodriguez, jalfonso}@ita.es

F. Rotella and F. J. Carrillo are with ENIT, Tarbes, France  
e-mail:{rotella, carrillo}@enit.fr

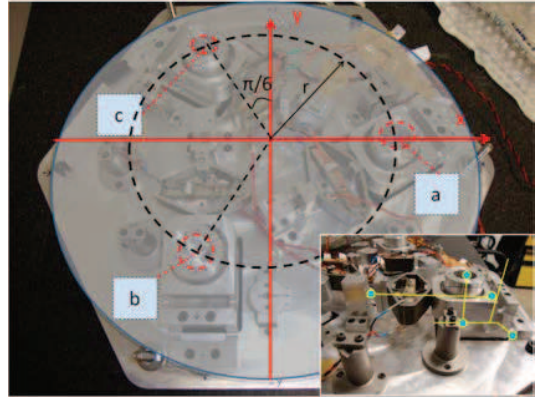


Fig. 1. Positioning platform used for the control implementation and detail of one actuation line.

## II. DESCRIPTION OF THE PLATFORM

The nanopositioning platform in the Figure 1 is intended for generating accurate displacements in  $z$  and rotations around  $x$  and  $y$  axes by means of the actuation lines  $a$ ,  $b$  and  $c$ . The actuation lines are shifted 120 degrees and follow the tripod structure described in [14]. The Figure 1 shows the detail of one actuation line  $j$ . The actuator between  $P_{1,j}$  and  $P_{2,j}$  moves parallel to the horizontal plane and the actuation direction is modified by the lever at  $P_{3,j}$ . The pillar between  $P_{4,j}$  and  $P_{5,j}$  transmits the vertical displacement to the upper platform.

The piezoelectric actuator APA-120ML from Cedrat Group is used. The only sensors available are three embedded strain gauge sensors in the actuation lines (from now on SGS).

### A. Mathematical description of the system

Although the proposed control does not need to have a detailed model of the system, the mathematical derivation of its representation is slightly outlined. The complete derivation can be found in [14]. This representation will permit to understand the assumptions considered for obtaining the *ultra-local* model in the Section 3. The system model is defined by:

- States: position ( $\mathbf{z}$ ), velocity ( $\dot{\mathbf{z}}$ ) of the upper platform in the three degrees of freedom, and charge ( $\mathbf{q}$ ) in the

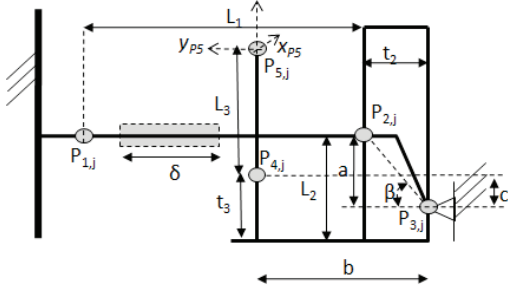


Fig. 2. Parameters of the actuation line  $j$  ( $j = a, b, c$ ).

three piezoelectric actuators:

$$\mathbf{z} = \begin{pmatrix} z \\ \theta_x \\ \theta_y \end{pmatrix}, \dot{\mathbf{z}} = \begin{pmatrix} \dot{z} \\ \dot{\theta}_x \\ \dot{\theta}_y \end{pmatrix}, \mathbf{q} = \begin{pmatrix} q_a \\ q_b \\ q_c \end{pmatrix} \quad (1)$$

From now on, subindices  $a, b$  and  $c$  refer to the actuation lines in the Figure 1.

- System inputs: the input voltage to the three actuators  $a, b$  and  $c$ :

$$\mathbf{v} = \begin{pmatrix} V_a \\ V_b \\ V_c \end{pmatrix} \quad (2)$$

The representation of the complete system is sequentially obtained by defining the behaviour of each single actuation line and finally coupling them using the rotation of the upper platform and the dynamic loads. In the actuation line  $j$  assuming small displacements of the actuator ( $\delta_j$ ), the angles  $\alpha_{i,j}$  of each joint  $P_{i,j}$  are (Figure 2):

$$\begin{aligned} \alpha_{1,j} &\approx \alpha_{5,j} \approx 0 \\ \alpha_{3,j} &\approx \frac{\delta_j}{t_4 \sin(\pi/2 - \beta)} \\ \alpha_{2,j} &\approx \alpha_{4,j} \approx \alpha_{3,j} \end{aligned} \quad (3)$$

With  $t_4 = \sqrt{t_2^2 + a^2}$ . The Figure 2 shows the main parameters of the line. The relationship between  $\delta_{p,j}$ , the deformation at a definite voltage if no load is applied on the actuator  $j$ , and the displacement ( $x_j$ ) is obtained as:

$$x_j = A_1 \delta_{p,j} - A_2 F_j \quad (4)$$

Where,

$$\begin{aligned} A_1 &= \frac{k_{e1} a_m b}{k_{e1} a a_m + (k_{b2} + k_{b3} + k_{b4})} \\ A_2 &= \left( \frac{1}{k_{e3}} + \frac{a_m b^2}{k_{e1} a^2 a_m + (k_{b2} + k_{b3} + k_{b4})} \right) \\ a_m &= t_4 \sin(\pi/2 - \beta) \\ k_{e1} &= \left( \frac{1}{k_{a1}} + \frac{1}{k_{a2}} + \frac{1}{k_p} \right)^{-1}, k_{e3} = \left( \frac{1}{k_{a4}} + \frac{1}{k_{a5}} \right)^{-1} \end{aligned} \quad (5)$$

In the expressions above,  $k_{e1}$  is the equivalent stiffness in the horizontal bar, and  $k_{e3}$  is the stiffness of the pillar.  $k_{ai}$

and  $k_{bi}$  represent the axial and rotation stiffness of joint  $i$ .  $k_p$  is the stiffness of the actuator. The free displacement of the piezoelectric actuator can be simplified as:

$$\delta_{p,j} = a_{pzt} q_j \quad (6)$$

Where  $a_{pzt}$  is the electromechanical transformation factor of the actuator (without considering hysteresis).

The force applied at the actuator  $j$  ( $F_{1,j}$ ) because of the displacement  $x_j$  and the load  $F_j$  is:

$$F_{1,j} = B_1 F_j + B_2 x_j \quad (7)$$

Where,

$$\begin{aligned} B_1 &= \frac{b}{a} + \frac{1}{b k_{e3} a_m} (k_{b2} + k_{b3} + k_{b4}) \\ B_2 &= \frac{1}{b a_m} (k_{b2} + k_{b3} + k_{b4}) \end{aligned} \quad (8)$$

The coupling between the three actuation lines is obtained by the relative transformation between the degrees of freedom of the platform and the vertical movement of the three actuation lines ( $a, b, c$ ):

$$\mathbf{f} = \mathbf{T}_f \mathbf{f}_{abc}, \mathbf{z} = (\mathbf{T}_f^T)^{-1} \mathbf{x}_{abc} \quad (9)$$

Where,

$$\begin{aligned} \mathbf{T}_f &= \begin{pmatrix} 1 & 1 & 1 \\ 0 & -r \cos(\pi/6) & r \cos(\pi/6) \\ -r & r \sin(\pi/6) & r \sin(\pi/6) \end{pmatrix} \\ \mathbf{f} &= \begin{pmatrix} F_z \\ \Gamma_x \\ \Gamma_y \end{pmatrix}, \mathbf{f}_{abc} = \begin{pmatrix} F_a \\ F_b \\ F_c \end{pmatrix}, \mathbf{x}_{abc} = \begin{pmatrix} x_a \\ x_b \\ x_c \end{pmatrix} \end{aligned} \quad (10)$$

$F_k$  and  $\Gamma_k$  stand for forces and torques in direction  $k$  ( $k = x, y, z$ ).

The coupling of the upper platform by the dynamic loads and the rotation angles  $\theta_x$  and  $\theta_y$  is:

$$\mathbf{f} = \mathbf{M} \ddot{\mathbf{z}} + \mathbf{C}_v \dot{\mathbf{z}} + \mathbf{D} \mathbf{z} \quad (11)$$

With,

$$\begin{aligned} \mathbf{M} &= \begin{pmatrix} M & 0 & 0 \\ 0 & J_x & 0 \\ 0 & 0 & J_y \end{pmatrix}, \mathbf{D} = \begin{pmatrix} 0 & \mathbf{0}_{1 \times 2} \\ \mathbf{0}_{2 \times 1} & -\mathbf{T}_{\alpha 5}^T \mathbf{K}_{\alpha 5} \mathbf{T}_{\alpha 5} \end{pmatrix} \\ \mathbf{C}_v &= \begin{pmatrix} c_{v,z} & 0 & 0 \\ 0 & c_{v,\theta_x} & 0 \\ 0 & 0 & c_{v,\theta_y} \end{pmatrix} \\ \mathbf{T}_{\alpha 5} &= \begin{pmatrix} \cos(\pi/3) & \cos(\pi/6) \\ -\sin(\pi/3) & \sin(\pi/6) \\ \cos(\pi/3) & -\cos(\pi/6) \\ \sin(\pi/3) & \sin(\pi/6) \\ -1 & 0 \\ 0 & -1 \end{pmatrix} \\ \mathbf{K}_{\alpha 5} &= \begin{pmatrix} \mathbf{k}_{b5} & \mathbf{0} & \mathbf{0} \\ \mathbf{0} & \mathbf{k}_{b5} & \mathbf{0} \\ \mathbf{0} & \mathbf{0} & \mathbf{k}_{b5} \end{pmatrix}, \mathbf{k}_{b5} = \begin{pmatrix} k_{b5,x} & k_{b5,xy} \\ k_{b5,xy} & k_{b5,y} \end{pmatrix} \end{aligned} \quad (12)$$

$\mathbf{M}$  stands for an inertia matrix in the three degrees of freedom (mass  $M$  and rotation inertias  $J_x$  and  $J_y$ ),  $c_{v,z}$ ,  $c_{v,\theta_x}$ ,  $c_{v,\theta_y}$  are the viscous friction terms in the three degrees of freedom, and  $\mathbf{D}$  is the stiffness associated with the link 5 (Figure 2).  $k_{b5,x}$ ,  $k_{b5,y}$  are the stiffness of the link 5 in the local axis (Figure 2),  $k_{b5,xy}$  is the coupled stiffness.  $\delta_{p,j}$  can be related with the electrical charge  $q_j$  in the actuator  $j$  (5) which depends on the input voltage by:

$$\dot{q}_j = \frac{1}{R_e} \left( V_j - \frac{q_j}{C} + a_{pzt} F_{1,j} \right) \quad (13)$$

where,

$V_j$  : voltage applied to the actuator  $j$  [V]  
 $q_j$  : charge in the piezoelectric capacitor  $j$  [C]  
 $R_e$  : electric resistance from amplifier to actuator [ $\Omega$ ]  
 $C$  : capacitance value of the actuator [F]

Combining (4), (7), (11) and (13) the obtained state space representation is:

$$\begin{aligned} \begin{pmatrix} \dot{\mathbf{z}} \\ \dot{\mathbf{q}} \end{pmatrix} &= \begin{pmatrix} \mathbf{0}_{3 \times 3} & \mathbf{1}_{3 \times 3} & \mathbf{0}_{3 \times 3} \\ -\mathbf{H}_1 & -\mathbf{H}_2 & -\mathbf{H}_3 \\ \mathbf{H}_4 & \mathbf{H}_5 & \mathbf{H}_6 \end{pmatrix} \begin{pmatrix} \mathbf{z} \\ \dot{\mathbf{z}} \\ \mathbf{q} \end{pmatrix} + \\ &\begin{pmatrix} \mathbf{0}_{3 \times 3} \\ \mathbf{0}_{3 \times 3} \\ \mathbf{H}_7 \end{pmatrix} \mathbf{v} \\ &= \mathbf{A}_{ss} \mathbf{x}_{ss} + \mathbf{B}_{ss} \mathbf{v} \end{aligned} \quad (14)$$

With,

$$\begin{aligned} \mathbf{H}_0 &= \mathbf{a}_{pzt} \mathbf{B}_1 \mathbf{T}_f^{-1} \\ \mathbf{H}_1 &= \left( \mathbf{A}_2 \mathbf{T}_f^{-1} \mathbf{M} \right)^{-1} \left( \mathbf{T}_f^T + \mathbf{A}_2 \mathbf{T}_f^{-1} \mathbf{D} \right) \\ \mathbf{H}_2 &= \left( \mathbf{A}_2 \mathbf{T}_f^{-1} \mathbf{M} \right)^{-1} \mathbf{A}_2 \mathbf{T}_f^{-1} \mathbf{C}_v \\ \mathbf{H}_3 &= \left( \mathbf{A}_2 \mathbf{T}_f^{-1} \mathbf{M} \right)^{-1} \mathbf{A}_1 \mathbf{a}_{pzt} \\ \mathbf{H}_4 &= \mathbf{R}_e^{-1} \left( \mathbf{a}_{pzt} \mathbf{B}_2 \mathbf{T}_f^T + \mathbf{H}_0 \mathbf{D} - \mathbf{H}_0 \mathbf{M} \mathbf{H}_1 \right) \\ \mathbf{H}_5 &= \mathbf{R}_e^{-1} \left( \mathbf{H}_0 \mathbf{C}_v - \mathbf{H}_0 \mathbf{M} \mathbf{H}_2 \right) \\ \mathbf{H}_6 &= \mathbf{R}_e^{-1} \left( -\mathbf{C}^{-1} - \mathbf{H}_0 \mathbf{M} \mathbf{H}_3 \right) \\ \mathbf{H}_7 &= \mathbf{R}_e^{-1} \end{aligned} \quad (15)$$

$\mathbf{A}_1$ ,  $\mathbf{A}_2$ ,  $\mathbf{B}_1$ ,  $\mathbf{B}_2$ ,  $\mathbf{R}_e$ ,  $\mathbf{C}$  and  $\mathbf{a}_{pzt}$  are diagonal matrices with the diagonal terms equal to the scalar value of the same name.

As observed in the previous expressions, the application of the complete mathematical model requires the knowledge of an important number of parameters: electrical and mechanical characteristics of the actuator; inertia, stiffness and damping in the different actuation lines and the upper platform; geometry of the lay-out. Many of these parameters are not easy to obtain, specially if the platform has been designed by an external supplier. This would be the case of the individual stiffness of the different flexures, or the exact dimensions of the different elements for obtaining the geometrical relationships. Other parameters are not available, even if the platform is designed and mounted by the same group, like the damping coefficients in the different degrees of freedom. And there is still another important factor

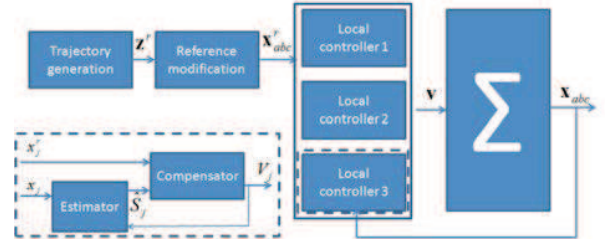


Fig. 3. Description of the control loop.

that complicates the availability of all the parameters in the model: the existence of nonlinearities and time-varying parameters. The most important examples are the hysteresis present in the actuators, and the coupling between the actuation lines. For all these reasons, a model-free control approach is specially appealing.

### III. MODEL-FREE CONTROL

A block diagram of the control strategy is shown in the Figure 3 and includes three local controllers, one for each actuation line. The control takes as input the reference trajectory  $\mathbf{x}^r$  and the displacement measured in the SGSs for calculating the control command. The displacement of the actuation line is estimated as:

$$x_j = k_{SGS} x_{SGS,j} \quad (16)$$

with  $k_{SGS}$  the gain of the sensor.

In order to transform the reference trajectory in the global coordinates  $\mathbf{z}^r$  to the local coordinates  $\mathbf{x}^r$ , the relationship (9) is used. The detail of the control implementation is given in the next subsections.

#### A. Local control of the actuation lines

The proposed control for each actuation line is an adaptive PI (a-PI) according to [10]. This approach is based on the so-called *ultra-local* representation which assumes that the system in a definite instant can be expressed as:

$$x_j^n = \alpha V_j + S_j \quad (17)$$

where,

$x_j^n$  :  $n$ -th derivative of the displacement of the  $j$  actuator, with  $j = a, b, c$  [ $m/s^n$ ]  
 $V_j$  : voltage command in the actuation line  $j$ , for  $j = a, b, c$  [V]  
 $\alpha$  : gain parameter representing the sensitivity of  $x_j^n$  to the input  $V_j$  [ $m/(s^n V)$ ]  
 $S_j$  : structural parameter of the unknown system, with  $j = a, b, c$  [ $m/s^n$ ]

As the three actuation lines are mechanically the same, the value of  $\alpha$  is assumed the same for the three of them. For the positioning platform, we define  $n = 1$ . To understand this selection and its limitations, we combine (4) and (6):

$$x_j = A_1 a_{pzt} q_j - A_2 F_j \quad (18)$$

By neglecting the direct piezoelectric effect (induced voltage due to mechanical loads), and assuming the electrical response time of the piezoelectric actuators much faster than the mechanical one, (13) can be simplified as:

$$V_j = \frac{q_j}{C} \quad (19)$$

And therefore (18) is rewritten as:

$$x_j = A_1 a_{pzt} C V_j - A_2 F_j \quad (20)$$

$F_j$  is calculated using (9) and (11). For slow movements, the acceleration term can be neglected and  $F_j$  results in:

$$F_j = (T_{f,ij})^{-1} \left( C_{v,ij} (T_{f,ij}^T)^{-1} \dot{x}_i + D_{ij} (T_{f,ij}^T)^{-1} x_i \right) \quad (21)$$

(21) can be rewritten as an *ultra-local* model with a constant parameter  $\alpha$ :

$$\begin{aligned} \dot{x}_j &= \alpha V_j + S_j \\ \alpha &= \frac{\dot{A}_1 a_{pzt} C}{(A_2 C_v)/9 + (4A_2 C_v)/(9r^2)} \end{aligned} \quad (22)$$

$S_j$  contains all the coupled terms from  $\dot{x}_i$  with  $i \neq j$ , and those related with  $x_j \forall j$  in (21).

The controller is an adaptive PI [10]:

$$V_j = \frac{1}{\alpha} \left( \dot{x}_j^r - \hat{S}_j + k_p (x_j^r - x_j) + k_i \int (x_j^r - x_j) dt \right) \quad (23)$$

Where  $\hat{S}_j$  is the estimation of  $S_j$  described in the next section.

The dynamics of the error  $e = (x^r - x)$  is obtained by substituting (23) into (22):

$$\dot{e}_j + k_p e_j + k_i \int e_j dt = 0 \quad (24)$$

Although the proportional term in (23) should be initially enough for obtaining good results as  $S_j$  contemplates internal perturbations, the experimental tests showed best performance using a PI compensator. The main reason seems to be that the integral term compensates possible errors in the estimation of  $S_j$  (sensor noise, ...).

#### IV. DESIGN METHODOLOGY

The controller design (23) is based on the following procedure:

- Identification of the order of the system by using a theoretical approach like in the Section 3.A or the gain estimator described in the Section 4.A.
- The estimation of the gain parameter  $\alpha$  can be done in three different ways:
  - By using a theoretically derived value (22).
  - Experimentally, by adjusting the value of the gain until having a good signal tracking with  $k_p = k_i = 0$  in (23). A combination of the theoretical one with a posterior experimental tuning is used for the positioning platform.

– With the estimator described in the Section 4.A.

- The estimation of the structural parameter  $S_j$  can be done by numerical differentiation or using perturbation observers.

##### A. Open loop gain estimator

An open-loop estimation algorithm for the parameter  $\alpha$  of (22) is described in this section. The estimated model of (22) is:

$$\hat{\dot{x}}_j = \hat{\alpha} V_j + \hat{S}_j \quad (25)$$

The model can be considered as the addition of two different terms:

$$\dot{x}_j = \dot{x}_{ph,j} + \dot{x}_{r,j} \quad (26)$$

Where,  $\dot{x}_{ph,j}$  and  $\dot{x}_{r,j}$  are the in-phase and the out-of-phase components with respect to the input command, respectively.

The phase shift is used during the identification process:

$$\begin{aligned} \dot{x}_{ph,j} &= \alpha V_j = G_w \left( \frac{\dot{x}_j}{V_j} \right) V_j \\ \dot{x}_{r,j} &= S_j \end{aligned} \quad (27)$$

With  $G_w$  a low-pass filter for selecting the in-phase components. To do that, the filter is applied to the signal  $\frac{\dot{x}_j}{V_j}$ .

Following the previous definitions, the estimation error in the actuation line  $j$  ( $e_{e,j}$ ) can be expressed as:

$$\dot{e}_{e,j} = \dot{e}_{e,ph,j} + \dot{e}_{e,r,j} \quad (28)$$

Where,

$$\begin{aligned} \dot{e}_{e,ph,j} &= (\alpha - \hat{\alpha}) V_j \\ \dot{e}_{e,r,j} &= S_j - \hat{S}_j \end{aligned} \quad (29)$$

For estimating  $\alpha$ :

$$\begin{aligned} \ddot{e}_{e,ph,j} &= (\dot{\alpha} - \dot{\hat{\alpha}}) V_j + (\alpha - \hat{\alpha}) \dot{V}_j \\ \dot{\alpha} &= 0 \\ (\alpha - \hat{\alpha}) &= \frac{\dot{e}_{e,ph,j}}{V_j} \end{aligned} \quad (30)$$

Therefore:

$$\ddot{e}_{e,ph,j} = -\dot{\hat{\alpha}} V_j + \frac{\dot{e}_{e,ph,j}}{V_j} \dot{V}_j \quad (31)$$

For solving the estimation of the parameter, the following adaptation law is defined:

$$\dot{\hat{\alpha}} = \frac{\dot{e}_{e,ph,j}}{V_j^2} \dot{V}_j + (k_p \dot{e}_{e,ph,j} + k_i e_{e,ph,j}) \frac{1}{V_j} \quad (32)$$

Where  $k_p^e$  and  $k_i^e$  are estimation constants. In the identification phase, the signal  $V_j$  is selected by the designer and therefore its derivative is known.

Including (32) in (31), the dynamics of the estimation error is obtained:

$$\ddot{e}_{e,ph,j} + k_p \dot{e}_{e,ph,j} + k_i e_{e,ph,j} = 0 \quad (33)$$

It is important to remark that the control algorithm (23) shows an important robustness to small variations in the estimation of  $\alpha$ .

The procedure described in the present section can also be used for identifying the order of the system: if no constant parameter  $\alpha$  is obtained and only oscillative behaviour



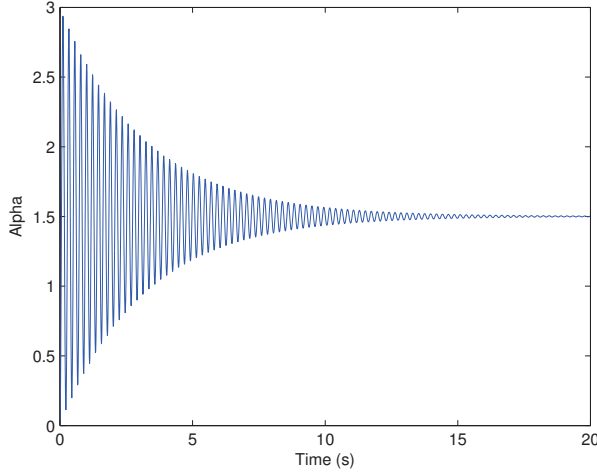


Fig. 4. Example of the on-line estimation algorithm.

is observed during the estimation, it is possible that the selected order should be higher in the analyzed dynamic range.

*Example 1.* As an example of the estimation procedure, the following model is identified:

$$\dot{y} = 1.5u + 50\sin(2\pi 100t + \pi/2)$$

For the estimation, the parameters below are used:

$$\begin{aligned} G_w &= \frac{1}{10s+1} \\ k_p &= 1256 \\ k_i &= 0 \end{aligned}$$

The estimator is working with a sample rate of 1kHz and a constant input  $u = 100$  is used during the process.

As it appears in the figure 4, the algorithm correctly estimates the value of  $\alpha$ .

### B. Estimation of the structural parameter

Two different options are analyzed for the estimation of the structural parameter  $S_j$  in (17):

- Numerical differentiation: the value of  $S_j$  is approached as:

$$S_j = \frac{1}{\tau s + 1} (k_{SGS} x_{SGS,j} s - \alpha V_j) \quad (34)$$

The first order filter is used for avoiding the high frequency amplification due to the numerical differentiation. Other options for this sort of approaches are the robust derivative estimations in [6].

- Perturbation estimation: the parameter  $S_j$  is considered as a external perturbation fulfilling (35):

$$\frac{dS_j}{dt} = 0, \forall j = a, b, c \quad (35)$$

(35) assumes that the sample time of the estimator is much lower than the response time of the system so that  $S_j$  is almost constant. According to this condition,

TABLE I  
PARAMETERS OF THE CONTROLLER

$\alpha$	$k_p$	$k_i$
-0.0023	20	20

it is possible to define an extended observer based on the following system:

$$\begin{aligned} \begin{pmatrix} \dot{x}_j \\ \dot{S}_j \end{pmatrix} &= \begin{pmatrix} 0 & 1 \\ 0 & 0 \end{pmatrix} \begin{pmatrix} x_j \\ S_j \end{pmatrix} + \begin{pmatrix} \alpha \\ 0 \end{pmatrix} V_j \\ &= \mathbf{A}_{j,es} \mathbf{x}_{j,v} + \mathbf{B}_{j,es} V_j \end{aligned} \quad (36)$$

Given the measure of  $x_j$ , the system is observable and the value of  $F_i$  can be estimated using a full state standard Luenberger observer:

$$\dot{\hat{\mathbf{x}}}_{j,v} = \mathbf{A}_{j,es} \hat{\mathbf{x}}_{j,v} + \mathbf{B}_{j,es} V_j + \mathbf{L}_j (x_j - \hat{x}_j) \quad (37)$$

The results described in the following section were obtained using numerical differentiation with a first order filter of 50Hz. The parameters of the controller (23) are listed in the table I. In this connection, it is important to remark that the sign of  $\alpha$  is negative because  $x_j$  decreases with positive voltage values.

## V. EXPERIMENTAL RESULTS

In this section, the behavior of the model-free controller is evaluated in the positioning platform described in the Section 2. The performance is evaluated in two different conditions:

- Static positioning.
- Dynamic trajectory tracking.

The following tests are obtained using an experimental test bench with the controllers implemented in a DS1103 controller board, which permits them to be directly imported from a Matlab Simulink model. For tuning the parameters of the controller, an interface programmed in DSpace ControlDesk software is used. The attached results are measurements from the embedded strain gauges in the three actuation lines.

### A. Static positioning

The Figure 5 shows the response of the system to a positioning reference in the different actuation lines. In stationary conditions, the model-free controller shows high positioning accuracy ( $< 0.02\mu m$ ) comparable to those of the much complex controller in [14].

### B. Dynamic trajectory tracking

The Figure 6 shows the tracking capabilities of the system for three different random signals commanded at the same time in the three actuation lines. At the sight of the results in the Figure 6 The model-free version works fine in slow movements ( $< 10\%$  at 2Hz) but its performance is limited by the first order approach in (22) which neglects the inertial terms.

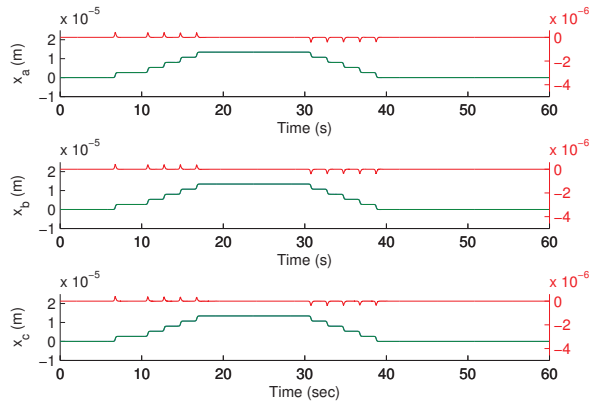


Fig. 5. Positioning pyramid-like movement (blue: measured position; green: reference signal; red: error).

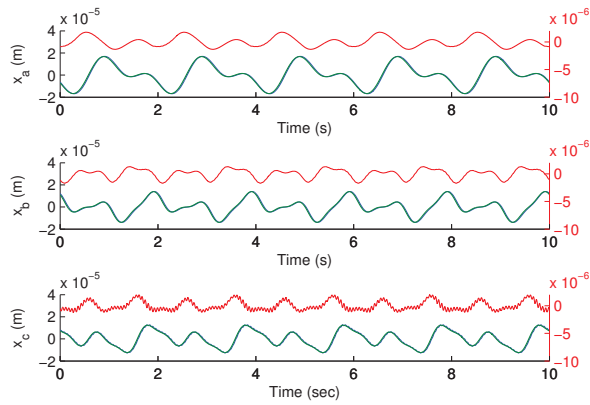


Fig. 6. Coupled movement of the three actuators (blue: measured position; green: reference signal; red: error).

## VI. CONCLUSIONS AND FUTURE WORK

The present work proves the capabilities of the model-free control strategy for handling systems with hysteresis and coupled behavior between actuators. In this connection, the proposed control represents an interesting option if no identified model is available or the conditions of the system could strongly change during the operation and no re-calibrating procedure is envisaged. The experimental evaluation shows error values below 0.1% in positioning applications, with higher values on increasing the dynamic requirements (error below 10% at  $2Hz$ ). This limitation is a result of the selected *ultra-local* representation which neglects inertial terms. Future activities could improve the system performance by applying the design methodology using higher order *ultra-local* representations.

The present work also proposes a design methodology for estimating the basic parameters of the controller: the order of the system, the  $\alpha$  gain and the structural parameter  $S$ . In this connection, it is remarkable a novel open-loop estimator for the gain parameter, which can also support the decision

on the order of the system.

## REFERENCES

- [1] B. M. Åkesson, H. T. Toivonen, "A neural network model predictive controller," *Journal of Process Control* 16 (2006). 937-946.
- [2] S. N. Balakrishnan, R. D. Weil, "Neurocontrol: A Literature Survey," *Mathl. Comput. Modelling* v.23:1/2 (1996). 101-117.
- [3] M. Fliess, C. Join, "Commande sans modèle et commande à modèle restreint," *e-STA*, v.5:4 (2008). 1-23.
- [4] M. Fliess, C. Join, "Model-free control and intelligent PID controllers: towards a possible trivialization of nonlinear control?," *Proc. of the 15th IFAC Symposium on System Identification (SYSID)*(2009).
- [5] M. Fliess, C. Join, S. Riachy, "Revisiting some practical issues in the implementation of model free control," *Proc. of the IFAC 18th World Congress* (2011).
- [6] M. Fliess, C. Join, H. Sira-Ramírez, "Non-linear estimation is easy," *Int. J. Model. Identif. Control*, v.4 (2008). 12-27.
- [7] J. Han, "From PID to Active Disturbance Rejection Control," *IEEE Trans. Industrial Electronics*, 56 (2009). 900-906.
- [8] P. Janssens, G. Pipeleers, J. Swevers, "Model-free iterative learning control for LTI systems and experimental validation on a linear motor test setup," *American Control Conference* (2011).
- [9] J. Levine, "Analysis and control of nonlinear systems: a flatness-based approach," Springer, 2009.
- [10] L. Michel, C. Join, M. Fliess, P. Sicard, A. Chériti, "Model-free control of dc/dc converters," *12th IEEE Workshop on Control and Modeling for Power Electronics* (2010).
- [11] L. Michel, "Model-free control of non-minimum phase systems and switched systems," *CoRR* abs/1106.1697 (2011).
- [12] L. Michel, "A unified model-free controller for switching minimum phase, non-minimum phase and time-delay systems," *CoRR* abs/1202.4707 (2012).
- [13] K. M. Passino, S. Yurkovich, "Fuzzy control," Addison Wesley (1998).
- [14] J. M. Rodriguez-Fortun, J. Orus, J. Alfonso, J. R. Sierra, F. Buil, F. Rotella, J. A. Castellanos, "Model-based design and control of a three-axis platform," *Mechatronics*, doi:10.1016/j.mechatronics.2012.06.004 (2012).
- [15] J. C. Spall, J. A. Cristion, "Model-free control of nonlinear stochastic systems with discrete-time measurements," *IEEE Transactions on Automatic Control*, v.43:9 (1998).
- [16] J. Villagra, B. Vinagre, I. Tejado, "Data-driven fractional PID control: application to DC motors in flexible joints," *IFAC Conference on Advances in PID Control* (2012).
- [17] J. Villagra, C. Balaguer, "A model-free approach for accurate joint motion control in humanoid locomotion," *International Journal of Humanoid Robotics* v. 8:1 (2011). 27-46.